EPJ Web of Conferences **3**, 03022 (2010)
DOI:10.1051/epjconf/20100303022

K^- ^{3}He and K^- ^{4}He interactions at low energies

V.Yu. Grishina[1,a]

Institute for Nuclear Research, 60th October Anniversary Prospect 7A, 117312 Moscow, Russia

Abstract. Using the multiple scattering approach (MSA) in the fixed center approximation we calculated the K^- ^{4}He and K^- ^{3}He scattering lengths. The K^- ^{4}He scattering length is also analyzed in the optical potential model. Within the MSA the K^- ^{3}He final state interaction factor was also calculated. It is found that the K^- ^{3}He mass spectrum for the $pd \to {}^3\mathrm{He}K^+K^-$ reaction is expected to be influenced by the K^- ^{3}He FSI effect.

1 Introduction

Low-energy $\bar{K}N$ and $\bar{K}A$ interactions have gained substantial interest during the last two decades. It is known from the time-honored Martin analysis [1] that the isoscalar S-wave K^-N scattering length is large and repulsive, Re a_0=−1.7 fm, while the isovector length is moderately attractive, Re a_1=0.37 fm. It is clear that such a strong repulsion in the KN isoscalar channel leads also to a repulsion in the low-energy K^-p system, since Re a_{K^-p}= 0.5 Re (a_0+a_1)=−0.66 fm. It should be noted that Conboy's analysis [2] of low energy $\bar{K}N$ data gives a solution with Rea_0=−1.03 fm and Re a_1=0.94 fm, that also results in repulsion in the K^-p channel, but with substantially smaller strength, Re a_{K^-p}=−0.05 fm. Recently, new data on the strong-interaction 1s level shift of kaonic hydrogen atoms were obtained at KEK (KpX experiment) [3,4] and Frascati (DEAR) [5]. They correspond to the following repulsive values of the K^-p scattering length

$$a(K^-p) = -(0.78 \pm 0.18) + i(0.49 \pm 0.37)\ \mathrm{fm} \qquad (1)$$

for KpX, and

$$a(K^-p) = (-0.468 \pm 0.090_{\mathrm{stat}} \pm 0.015_{\mathrm{syst}}) + i(0.302 \pm 0.135_{\mathrm{stat}} \pm 0.036_{\mathrm{syst}})\ \mathrm{fm} \qquad (2)$$

for DEAR. However, the consistency of the bound state with the scattering data can be questioned, as first pointed out in Ref. [6]. Nevertheless, it is possible that the actual K^-p interaction is attractive if the isoscalar $\Lambda(1405)$ resonance is a bound state of $\bar{K}N$ system [7,8]. A fundamental reason for such a scenario is provided by the leading order term in the chiral expansion for the K^-N amplitude which is attractive. The combination of chiral $SU(3)$ effective field theory with coupled channels was introduced. The starting point of this approach is the chiral effective Lagrangian which describes the coupling of the pseudoscalar meson octet (π, K, η) to the ground state baryon octet (N, Λ, Σ, Ξ). New developments in the analysis of the $\bar{K}N$ interaction based on chiral Lagrangians can be found in Refs. [9–13]. These results provide further support for the description of the $\Lambda(1405)$ as a meson-baryon bound state. More recently, it has even been argued that there are indeed two poles in the complex plane in the vicinity of the nominal $\Lambda(1405)$ pole [14]. For more recent evidence to support this scenario, see *e.g.* [15]. A different view seems to be taken in Ref.[16].

Such a non-trivial dynamics of the $\bar{K}N$ interaction leads to very interesting in-medium phenomena in interactions of anti-kaons with finite nuclei as well as with dense nuclear matter, including neutron stars, see *e.g.* Refs. [17–22].

Recently, exotic few-body nuclear systems involving the $\bar{K}$-meson as a constituent were studied by Akaishi and Yamazaki [23]. They proposed a phenomenological $\bar{K}N$ potential model, which reproduces the K^-p and K^-n scattering lengths from the Martin analysis [1], the kaonic hydrogen atom data from KEK [3,4] and the mass and width of the $\Lambda(1405)$ resonance. The KN interaction in this model is characterized by a strong I=0 attraction, which allows the few-body systems to form dense nuclear objects. As a result, the nuclear ground states of a K^- in (pp), ^{3}He, ^{4}He and ^{8}Be were predicted to be discrete states with binding energies of 48, 108, 86 and 113 MeV and widths of 61, 20, 34 and 38 MeV, respectively. More recent work on this subject can be found e.g. in Refs. [24,25].

Furthermore, recently a strange tribaryon $S^0(3115)$ was detected in the interaction of stopped K^--mesons with ^{4}He [26]. Its width was found to be less than 21 MeV. In principle, this state may be interpreted as a candidate of a deeply bound state $(KNNN)^{Z=0}$ with I=1, I_3=−1. However, the observed tribaryon $S^0(3115)$ is about 100 MeV lighter than the predicted mass. Moreover, in the experiment an isospin 1 state was detected at a position where no peak was predicted. It was discussed in Ref. [27] that such discrepancy can be resolved by improvement of the model [23]. The results of Akaishi and Yamazaki [23] were criticized by Oset and Toki [28] who argued that the model of Ref. [23] is unrealistic. Oset and Toki also suggested

[a] e-mail: grishina@cpc.inr.ac.ru

that the peaks in the reaction with ^{4}He can be due to K^- absorption on a pair of nucleons. This suggestion puts doubt whether a narrow tribaryon $S^0(3115)$ really exists.

Another tentative evidence for a K^-pp bound state produced in K^- absorption at rest on different nuclear targets was found by the FINUDA collaboration [29]. It was detected through its two-body decay into a Λ and a proton. The signal in the Λp invariant-mass distribution is about 115 MeV below the expected mass of the Λp system in case of non-bound K^-NN absorption. Magas *et al.* [30] showed that the FINUDA signal can also be explained by a $K^-pp \to \Lambda p$ reaction followed by final-state interactions (FSI) of the produced particles with the remnant nucleus. Therefore, the experimental claim for the formation of very deeply bound antikaonic nuclear systems recieve an alternative explanation in terms of conventional nuclear processes [31].

Thus, it is obvious that further searches for bound kaonic nuclear states as well as new data on the interactions of $\bar{K}$-mesons with light nuclei are of great interest.

The calculations of the K^-d scattering length were performed using the multiple scattering approach [32–34] in the fixed center approximation and Faddeev equations as well [33,35]. Futhermore, in Ref. [36] it was proposed the idea of extraction of the S-wave kaon-nucleon scattering lengths a_0 and a_1 from a combined analysis of existing kaonic hydrogen and synthetic deuterium data. In the framework of the low-energy effective field theory the restrictions on the values of the scattering lengths a_I, I=0,1 were obtained and the domain of the ReA_{Kd} and ImA_{Kd} values was found where solutions for a_0 and a_1 exist.

Up to now the S-wave K^- ^{4}He and K^- ^{3}He scattering lengths, which we respectively denote as $A(K^-\,^4\mathrm{He})$ and $A(K^-\,^3\mathrm{He})$, have not been measured. The first theoretical calculations of $A(K^-\,^4\mathrm{He})$ and $A(K^-\,^3\mathrm{He})$ within the framework of the multiple scattering approach (MSA) have been done in Refs. [37,38].

Furthermore, we discuss a possibility to measure the K^- ^{3}He scattering length through the K^- ^{3}He final state interaction (FSI) [38]. Recently we proposed to analyse the reaction $p\mathrm{d}\to {}^3\mathrm{He}K^+K^-$ near the threshold measured at COSY-Jülich [39]. We apply our approach to calculate the K^- ^{3}He FSI effect in this reaction and demonstrate that the K^- ^{3}He invariant mass distribution is sensitive enough to the K^- ^{3}He FSI and may be used for a determination of the S-wave K^- ^{3}He scattering length.

It should be mentioned that in Ref. [40] it was predicted that the $\bar{K}^0$d mass spectrum of the reaction $pp \to \mathrm{d}K^+\bar{K}^0$ could be influenced by the $\bar{K}$d FSI effect. In recent analysis of the data on the $pp \to \mathrm{d}K^+\bar{K}^0$ reaction at Q=48 and 105 MeV it was found evidence of the FSI effect in the $\bar{K}^0$d system [41].

Our paper is organized as follows: In Sect. 2 we describe the K^- ^{4}He and K^- ^{3}He using multiple scattering approach in the fixed center approximation. In Sect. 3 we calculate the K^- ^{4}He and K^- ^{3}He scattering lengths within the MSA. We also obtain the $A(K^-\,^3\mathrm{He})$ using the optical potential model. In Sect. 4 an analysis of the FSI in the reaction $p\mathrm{d}\to {}^3\mathrm{He}K^+K^-$ near the threshold is considered. Our conclusions are given in Sect. 5.

2 K^-He interaction within the multiple-scattering approach

To calculate the S-wave K^-He scattering length as well as the FSI enhancement factor, we use the Multiple Scattering (MS) formalism [42]. Note that this method has already been used for the calculation of the enhancement factor in the reactions $p\mathrm{d}\to {}^3\mathrm{He}\eta$ [43], $pn\to \mathrm{d}\eta$ [44] and $pp\to \mathrm{d}K^0K^+$ [34].

The continuum wave function of the kaon, which is defined at fixed coordinates of the A = 4 or 3 nucleons in ^{4}He or ^{3}He, can be written as the sum of the incident plane wave of the kaon and waves emerging from the A fixed scattering centers. Keeping only the S-wave contribution, we can express the total wave function Ψ_k through the wave functions $\psi_j(\mathbf{r}_j)$ defined in each scattering center j in the following way

$$\Psi_k(\mathbf{r}_{K^-};\mathbf{r}_1,\mathbf{r}_2,\dots\mathbf{r}_A)=\mathrm{e}^{i\mathbf{k}\cdot\mathbf{r}_{K^-}}+\sum_{j=1}^{A}\tilde{f}_{K^-N_j}\frac{\mathbf{e}^{ikR_j}}{R_j}\,\psi_j(\mathbf{r}_j)\,, \quad (3)$$

where $R_j=\left|\mathbf{r}_{K^-}-\mathbf{r}_j\right|$ and the elastic scattering amplitude f_{K^-N} should be corrected by the factor proportional to the K^-N reduced mass [44,34]

$$\tilde{f}_{K^-N}(k_{K^-N}) = (1+\frac{m_{K^-}}{m})\,f_{K^-N}(k_{K^-N}) \quad (4)$$

with m (m_{K^-}) the nucleon (charged kaon) mass, and $k_{\bar{K}N}$ is the modulus of the relative $\bar{K}N$ momentum. Note that we use the unitarized scattering length approximation for the latter, *i.e.*

$$f^I_{\bar{K}N}(k_{\bar{K}N}) = \left[(a^I_{\bar{K}N})^{-1} - ik_{\bar{K}N}\right]^{-1}\,, \quad (5)$$

where I is the isospin of the $\bar{K}N$ system. For each scattering center j an effective wave $\psi_j(\mathbf{r}_j)$ is defined as the sum of the incident plane wave and the waves scattered from the $(A-1)$ other centers

$$\psi_j(\mathbf{r}_j) = \mathrm{e}^{i\mathbf{k}\cdot\mathbf{r}_j} + \sum_{l\neq j}\tilde{f}_{K^-N_l}\frac{\mathbf{e}^{ikR_{jl}}}{R_{jl}}\,\psi_l(\mathbf{r}_l)\,, \quad (6)$$

where $R_{jl}=\left|\mathbf{r}_l-\mathbf{r}_j\right|$. Therefore, the channel wave functions $\psi_j(\mathbf{r}_j)$ can be found by solving the system of the four linear equations (6).

To obtain the FSI factor we calculate the total wave function Ψ_k given by Eq. (3) at $\mathbf{r}_{K^-}=\sum_{j=1}^{A}\mathbf{r}_j$=0 and average it over the coordinates of the nucleons $\mathbf{r}_j$ in ^{4}He and ^{3}He. Thus the FSI enhancement factor is [42]

$$\lambda^{\mathrm{MS}}(k_{K^-\mathrm{He}})=\left|\left\langle\Psi_{q^{\mathrm{lab}}_{K^-}}(\mathbf{r}_{K^-}=\sum_{j=1}^{A}\mathbf{r}_j=0;\mathbf{r}_1,\mathbf{r}_2,\dots,\mathbf{r}_A)\right\rangle\right|^2. \quad (7)$$

For the nuclear density function we use the factorized form

$$|\Phi(\mathbf{r}_1,\mathbf{r}_2,\dots,\mathbf{r}_A)|^2 = \prod_{j=1}^{A}\rho_j(\mathbf{r}_j)\,, \quad (8)$$

where the single nucleon density is taken in Gaussian form as

$$\rho(\mathbf{r}) = \frac{1}{(\pi R^2)^{3/2}}\, \mathrm{e}^{-r^2/R^2} \qquad (9)$$

with $R^2/4 = 0.62$ and 0.7 fm^2 for ^{4}He and ^{3}He, respectively. Note, that the independent particle model gives a rather good description of the ^{4}He and ^{3}He electromagnetic form factors up to a momentum transfer $\mathbf{q}^2 = 8$ fm^{-2} (see *e.g.* Ref. [45]).

The integration in Eq. (7) over the nucleon coordinates $\mathbf{r}_j$ was performed using the Monte-Carlo method. This approach provides us with a possibility to include all configurations of the nucleons in ^{4}He and ^{3}He. Within this method we can also take into account in Eq. (3) the dependence of the $\tilde{f}_{K^-N_j}$ amplitude on the type of nucleonic scatterer, *i.e.* proton or neutron. Note that the simple version of the multiple scattering approach used in Ref. [46] can be applied only to the case of identical scatterers.

The S-wave K^-A scattering length can be derived from the asymptotic expansion of Eq. (3) at $r_{K^-}\to\infty$ and it is

$$A(K^-A) = \frac{m_{\mathrm{He}}}{m_{\mathrm{He}} + m_{K^-}} \left\langle \sum_{j=1}^{A} \tilde{f}_{K^-N}\, \psi_j(\mathbf{r}_j) \right\rangle \Bigg|_{\sum_{j=1}^{A} \mathbf{r}_j = 0} , \qquad (10)$$

with m_{He} the He-particle mass. Here the procedure of averaging over the coordinates of the nucleons is similar to that in Eq. (7).

3 The S-wave K^- ^{3}He and K^- ^{4}He scattering lengths

3.1 $A(K^-\,{}^4\mathrm{He})$ and $A(K^-\,{}^3\mathrm{He})$ calculations within the Multiple Scattering Approach

In order to calculate the S-wave K^- ^{3}He and K^- ^{4}He scattering lengths we use the multiple scattering approach (MSA) described in detail in the previous Sect. 2 of the present paper. The theoretical predictions for the K^- ^{4}He and K^- ^{3}He scattering lengths, $A(K^-\,{}^4\mathrm{He})$ and $A(K^-\,{}^3\mathrm{He})$, have been published in Refs. [48,37,38].

The basic uncertainties of the MSA calculations are given by the next-to-leading order model corrections such as recoil corrections, contributions from inelastic double and triple scattering terms, *etc.* and due to the uncertainties of the elementary I=0 and I=1 $\bar{K}N$ scattering lengths. It should be noted that problem of the recoil corrections was recently studied for the $\bar{K}$d scattering in the framework of the effective field theory [47]. Due to specific cancellations the net recoil effect for the double-scattering process is found to be just about $10-15\%$ of the static contribution.

In the present work the calculations of the K^- ^{4}He and K^- ^{3}He scattering length were done in the fixed center approximation. Five sets of parameters for the $\bar{K}N$ lengths are shown in the Table 1. We consider the $\bar{K}N$ scattering lengths from a K-matrix fit (Set 1) [32] as well as the predictions for the $\bar{K}N$ scattering amplitudes based on the chiral unitary approach of Ref. [11] (Set 2). The constant scattering-length fit from Conboy [2] is denoted as Set 3. We note that the $\bar{K}N$ scattering lengths described by Sets 1–3 correspond to their vacuum values. At the same time Sets 4–5 describe the effective $\bar{K}N$ scattering lengths that contain in-medium effects.

One of the most extensive analyses of the effective $\bar{K}N$ interactions in nuclear medium has been presented by Ramos and Oset [49] within a self-consistent microscopic theory. The resulting K^- attraction in medium has been found to be smaller than predicted by other theories and approximation schemes. The isospin-averaged effective $\bar{K}N$ scattering length is moderately attractive and its real part does not exceed the value of

$$\mathrm{Re}\, a^{\mathrm{eff}} \simeq 0.3\,\mathrm{fm}\,, \qquad (11)$$

at nuclear density $\rho \geq 0.3\rho_0$. The obtained shallow K^--nucleus optical potential with a depth of -50 MeV (for the real part of the potential at $\rho = \rho_0$) was successfully used to reproduce the experimental shifts and widths of kaonic atoms over the periodic table [50].

In contrast to the results of Ref. [49], Akaishi and Yamazaki [23] proposed much more attractive optical potential which corresponds to the following effective $\bar{K}N$ scattering lengths for the $I = 0, 1$ channels in the nuclear medium

$$\begin{aligned} a_0^{\mathrm{eff}} &= 2.9 + i1.1\,\mathrm{fm}\,, \\ a_1^{\mathrm{eff}} &= 0.43 + i0.30\,\mathrm{fm}\,. \end{aligned} \qquad (12)$$

According to the Akaishi and Yamazaki approach, such a strong attraction appears already in the case of few-nucleon systems generating deeply bound $\bar{K}$-nuclear states [23].

In order to demonstrate the sensitivity of our results to possible modifications of the $\bar{K}N$ scattering amplitudes in the presence of nuclei we consider as Set 4 the moderately attractive effective scattering length from Ref. [49]. As Set 5 we choose the strongly attractive in-medium solution found in Refs. [23,27] and given by Eq.(12).

The calculated values of $A(K^{-4}\mathrm{He})$ and $A(K^-\,{}^3\mathrm{He})$ are listed in the last two columns of Table 2. They are very similar for Sets 1 and 2, $A(K^{-4}\mathrm{He}) \sim (-1.9 + i1.0)$ fm and $A(K^-\,{}^3\mathrm{He}) \sim (-1.6 + i1.0)$ fm. The results for Set 3 are quite different especially for the imaginary part of $A(K^-\,{}^3\mathrm{He})$ and the real part of $A(K^{-3}\mathrm{He})$. The calculations with the effective $\bar{K}N$ amplitude from Ref. [49] give the K^{-4}He scattering length with an imaginary part roughly two times larger than the result obtained with the vacuum $\bar{K}N$ scattering lengths. Not surprisingly, the exotic Set 5 for the elementary amplitudes extracted from Refs. [23,27] leads to enormously large scattering lengths for K^- ^{4}He and K^- ^{3}He systems with real parts of -3.5 fm and -4 fm, respectively. In the case of Set 5 we also performed calculations using the single-nucleon density parameters in Eq. (9) from Ref. [23] $R^2/4 = 0.48$ and 0.64 fm^2 for ^{4}He and ^{3}He, respectively. The obtained results $A(K^-\mathrm{He}) = -2.99 + i1.27$ fm and $A(K^-\,{}^3\mathrm{He}) = -3.91 + i3.62$ fm are not very different for the real parts of the scattering lengths.

Table 1. Various sets of the elementary $\bar{K}N$ scattering lengths $a_I(\bar{K}N)$ ($I = 0, 1$). Sets 1–3 correspond to their vacuum values. The Sets 4–5 describe the effective $\bar{K}N$ scattering lengths that contain in-medium effects.

Description	Set	$a_0(\bar{K}N)$ [fm]	$a_1(\bar{K}N)$ [fm]
1	[32]	$-1.59 + i0.76$	$0.26 + i0.57$
2	[11]	$-1.31 + i1.24$	$0.26 + i0.66$
3	[2]	$-1.03 + i0.95$	$0.94 + i0.72$
4	[49]	$0.33 + i0.45$ isospin average	
5	[23]	$2.9 + i1.1$	$0.43 + i0.30$

Table 2. K^- ^{4}He and K^- ^{3}He scattering lengths for various choices of the elementary $\bar{K}N$ scattering lengths $a_I(\bar{K}N)$ ($I = 0, 1$). The effective $\bar{K}N$ scattering length of Set 4 is extracted from the isospin averaged optical potential. Therefore it can only be applied for the calculation of $A(K^-$ ^{4}He).

Set	$A^{\rm MS}(K^-$ ^{4}He) [fm]	$A^{\rm MS}(K^-$ ^{3}He) [fm]	$A^{\rm opt}(K^-$ ^{4}He) [fm]
1	$-1.80 + i0.90$	$-1.50 + i0.83$	$-1.26 + i0.60$
2	$-1.98 + i1.08$	$-1.66 + i1.10$	$-1.39 + i0.65$
3	$-2.24 + i1.58$	$-1.52 + i1.80$	$-1.59 + i0.88$
4	$-1.47 + i2.22$		$-1.51 + i1.20$
5	$-3.49 + i1.80$	$-3.93 + i4.03$	$-1.57 + i0.74$

3.2 $A(K^-$ ^{4}He) calculations within the optical potential model

Alternatively we applied the optical potential

$$V_{\rm opt}^{K^-A}(\mathbf{r}) = -\frac{2\pi}{\mu_{\bar{K}N}}\left[a_{K^-p}\,Z\rho_p(r) + a_{K^-n}N\rho_n(r)\right], \quad (13)$$

where $\mu_{\bar{K}N}$ is the reduced mass of the $\bar{K}N$ system and the single proton and neutron densities are $\rho_p(r) = \rho_n(r) = \rho(r)$ defined by Eq. (9) with eliminated c.m. motion, *i.e.*, $R^2 \to R^2\,(A-1)/A$. The results for $A^{\rm opt}(K^-$ ^{4}He) are presented in the last column of Table 2. $A^{\rm opt}(K^-$ ^{4}He) was found to be about 30 – 40 % smaller then $A^{\rm MS}(K^-$ ^{4}He) for the vacuum parameters of the $\bar{K}N$ interactions. In the case of Set 5 the K^- ^{4}He scattering length calculated in the optical potential model is more than factor of two smaller than the result obtained in the framework of the MSA.

The single-scattering term of the total K^-A scattering length is the same in both the multiple scattering and optical-potential schemes. It is equal to

$$A^{(1)}(K^-A) = \frac{\mu_{\bar{K}A}}{\mu_{\bar{K}N}}\,(N\,a_{\bar{K}n} + Z\,a_{\bar{K}p})\,,$$

where $\mu_{\bar{K}A}$ is the K^-A reduced mass. Note that in the case of the K^-d system the higher order rescattering corrections were analyzed within the fixed center approximation to the Faddeev equations with the input parameters from the chiral unitary approach [35]. Their contributions were evaluated and were found to be very noticeable. Within the optical-potential model the next-to-leading order scattering terms $A^{(n)}(K^-A)$ are defined by using different procedures of averaging over the coordinates of the nucleons than in the case of the MSA in the fixed center approximation. However, the total meson-nucleus scattering length obtained within the simplest optical-potential model needs some corrections, which are especially important for few-body systems. Particularly, in Ref. [46] the isospin-symmetric case of the η-nucleus system was considered with equal elementary scattering amplitudes of the η meson on the proton and neutron. For the η-nucleus scattering length calculated by use of the optical-potential model it was suggested that each multiple-scattering term of n-th order should be corrected by a factor $[(A-1)/A]^n$ to remove multiple collisions on the same nucleon. Such a correction cannot be used for the K^-A optical-potential calculations because of the significantly different K^-n and K^-p scattering lengths. The advantage of the MSA applied to the K^-A system is that it explicitely takes into account the difference between the elementary K^-p and K^-n scattering amplitudes. Furthermore, if the $\bar{K}N$ interaction radius is small compared to the size of the nucleus, *i. e.* $R_{\rm int} \leq 1$ fm, the MSA is valid and the overall scattering amplitude can be expressed in terms of the individual on-shell meson-nucleon amplitudes without extra free parameters.

4 K^- ^{3}He final state interaction in $pd \to {}^3{\rm He}\,K^+K^-$ reaction

We now discuss the K^- ^{3}He FSI effect in the reaction $pd \to {}^3{\rm He}\,K^+K^-$ near threshold and compare our calculations with the data from the MOMO experiment [39] at COSY-Jülich. The MOMO collaboration measured at three different beam energies, corresponding to excess energies of $Q = 35,\ 41$ and 55 MeV with respect to the K^+K^- threshold. We only consider the data at the central energy since these constitute the best compromise between available phase space and resolution for our analyses. The MOMO data are presented in terms of relative energies $T_{K^-\,^3{\rm He}}$ and $T_{K^+K^-}$; in the non-relativistic approximation they can be expressed through the corresponding invariant masses M_{ij} by $T_{ij} = M_{ij} - m_i - m_j$. Since the MOMO experiment was not sensitive to the charge of the detected kaons, the measured $T(K,\ ^3{\rm He})$ distributions (see Fig. 2) are symmetric with respect to $T(K,\ ^3{\rm He}) = Q/2$. This is taken into account in our calculations by constructing the half-sum of the K^+ and K^- contributions.

As the first step of our analysis we neglect all FSI effects and investigate the contribution of the $\phi(1020)$ meson by fitting the K^+K^- relative-energy distribution (taking into account the experimental mass resolution quoted in Ref. [39]). The ϕ-meson contribution is found to be about 16% of the total cross section (9.6 ± 1.0) nb, which is in agreement with the result from Ref. [39]. In Fig. 1 we show the K^+K^- relative-energy distribution; the solid line describes the incoherent sum of a pure phase-space distribution and the $\phi(1020)$ contribution.

The K^- ^{3}He FSI effect could influence the non-ϕ contribution to the $pd \to {}^3{\rm He}K^+K^-$ reaction. It should be noted, that the $\phi(1020)$-meson most probably decays into the K^+K^- pairs outside the nucleus and these kaons practically do not interact with the ^{3}He system. Within the MSA we calculated the FSI enhancement factor for the K^- ^{3}He system.

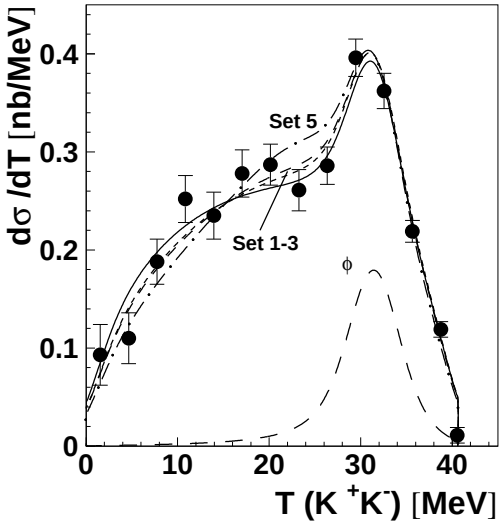

Fig. 1. Distribution of the the K^+K^- relative energy for the $p\mathrm{d} \to {}^3\mathrm{He}\,K^+K^-$ reaction at an excess energy of 41 MeV. The MOMO data are taken from Ref. [39]. The solid line describes the incoherent sum of a pure phase-space distribution and the $\phi(1020)$ contribution (long-dashed line). The short-dashed and dashed lines show the effect of the $K^-\,{}^3\mathrm{He}$ FSI for parameters of Set 1 and 3, respectively. The dash-dotted line shows the effect for the strongly modified $\bar{K}N$ scattering lengths in nuclear medium [23] leading to the deeply bound states.

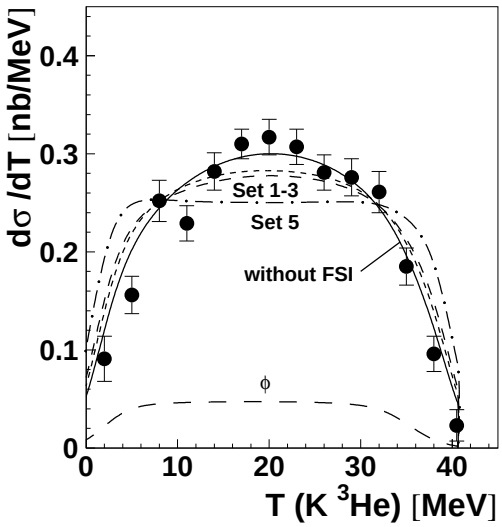

Fig. 2. Distribution of the $K\,{}^3\mathrm{He}$ relative energy for the $p\mathrm{d} \to {}^3\mathrm{He}\,K^+K^-$ reaction at an excess energy of 41 MeV. The MOMO data are taken from Ref. [39]. The solid line describes the incoherent sum of a pure phase-space distribution and the $\phi(1020)$ contribution (long-dashed line). The short-dashed and dashed lines show the effect of the $K^-\,{}^3\mathrm{He}$ FSI for parameters of Set 1 and 3, respectively. The dash-dotted line shows the effect for the strongly modified $\bar{K}N$ scattering lengths in nuclear medium [23] leading to the deeply bound states.

The short-dashed and dashed lines in Fig. 1 show the influence of the $K^-\,{}^3\mathrm{He}$ FSI on the K^+K^- relative-energy distribution. The dash-dotted line shows the effect for the

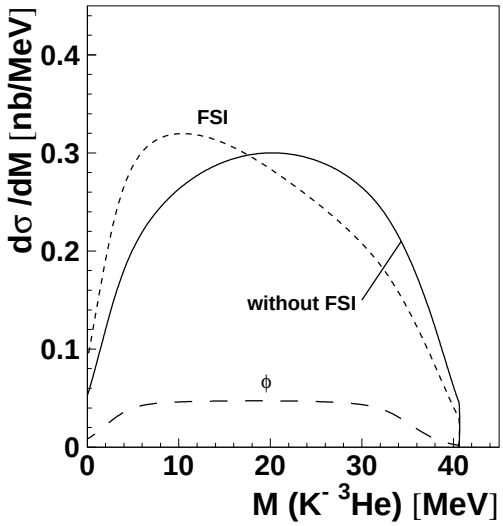

Fig. 3. The $K^-\,{}^3\mathrm{He}$ mass distribution for the $p\mathrm{d} \to {}^3\mathrm{He}\,K^+K^-$ reaction at an excess energy of 41 MeV. The solid line describes the incoherent sum of a pure phase-space distribution and the $\phi(1020)$ contribution (long-dashed line). The short-dashed line shows the effect of the $K^-\,{}^3\mathrm{He}$ FSI calculated for parameters of Set 1.

strongly modified $\bar{K}N$ scattering lengths in nuclear medium (Set 5) leading to the deeply bound states.

In Fig. 2 we also present calculations of the $K\,{}^3\mathrm{He}$ relative-energy spectrum. However the signs of charges of two kaons were not determined in the MOMO vertex detector. As a consequence, for the $K^3\mathrm{He}$ relative energy distribution the $K^-\,{}^3\mathrm{He}$ FSI effect is averaged over the two charge states of K^- and K^+. The predictions are normalized to the total $p\mathrm{d} \to {}^3\mathrm{He}\,K^+K^-$ cross section of 9.6 nb. The dash-dotted line, corresponding to Set 5, demonstrates a pronounced deformation of the $K\,{}^3\mathrm{He}$ relative-energy spectrum. It is in clear contradiction to the data.

While the solution without FSI is in best agreement with the data, the results with $K^-\,{}^3\mathrm{He}$ FSI calculated using elementary $\bar{K}N$ amplitudes from Sets 1–3 cannot be ruled out due to the uncertainties of the MSA (see *e.g.* Ref. [37, 38]) and the experimental errors.

From the other hand, as it is seen in Fig. 3 we expect that the $K^-\,{}^3\mathrm{He}$ FSI effect leads to rather strong enhancement at low masses of the $K^-\,{}^3\mathrm{He}$ invariant mass spectrum for the $p\mathrm{d} \to {}^3\mathrm{He}K^+K^-$ reaction near threshold. In order to advance the understanding of the $K^-\,{}^3\mathrm{He}$ FSI new measurements of the the reaction $p\mathrm{d} \to {}^3\mathrm{He}K^+K^-$ near threshold to be carried out with identification of all three final state particles.

5 Conclusions

We present predictions for the $K^-\,{}^3\mathrm{He}$ and $K^-\,{}^4\mathrm{He}$ scattering lengths obtained within the framework of the Multiple Scattering Approach. We have studied uncertainties of the

calculations due to the presently available elementary K^-N scattering lengths. The predicted values are $A(K^-\,^3\mathrm{He}) = -(1.5 \div 1.7) + i(0.8 \div 1.1)$ fm and $A(K^-\,^4\mathrm{He}) = -(1.8 \div 2.0) + i(0.9 \div 1.1)$ fm for the vacuum $\bar{K}N$ amplitudes. The estimates with the exotic values for the input elementary $\bar{K}N$ amplitudes extracted from the deep optical potential proposed by Akaishi and Yamazaki [23] give enormously large scattering lengths $A(K^-\,^4\mathrm{He})$ and $A(K^-\,^3\mathrm{He})$ with real parts of -3.5 and -4 fm, respectively. We have also calculated the $A(K^-\,^4\mathrm{He})$ using the optical potential model. We have analyzed the $K^-\,^3$He final-state interactions in the reaction $p\mathrm{d} \to {}^3\mathrm{He}\,K^+K^-$ near threshold and compare our model calculations with the existing data from the MOMO collaboration at COSY-Jülich accelerator [39]. For the $K^-\,^3$He invariant mass spectrum of the $p\mathrm{d} \to {}^3\mathrm{He}K^+K^-$ reaction near threshold we expect that the $K^-\,^3$He FSI effect leads to rather strong enhancement at low masses of the $K^-\,^3$He system.

6 Acknowledgments

I am grateful to M. Büscher, L.A. Kondratyuk and A. Dzyuba for collaboration on the problem of interactions of the low-energy antikaons with lightest nuclei. It is pleasure to thank C. Wilkin, A.E. Kudryavtsev, A. Sibirtsev, V. Baru, S. Krewald, J. Haidenbauer and H. Ströher for fruitful discussions. This work was supported by DFG Grant No. 436 RUS 113/940/0.

References

1. A.D. Martin, Nucl. Phys. B, Phys. Rev. **179** (1981) 33
2. J.E. Conboy, Rutherford-Appleton Lab. Report, RAL-85-091 (1985)
3. T.M. Itoh *et al.*, Phys. Rev. C **58** (1998) 2366
4. M. Iwasaki *et al.*, Phys. Rev. Lett. **78** (1997) 3067
5. C. Guaraldo *et al.*, Eur. Phys. J. A **19** (2004) 185
6. U.-G. Meißner, U. Raha, A. Rusetsky, Eur. Phys. J. C **35**, (2004) 349
7. R. H. Dalitz, T. C. Wong, G. Rajasekaran, Phys. Rev. **153** (1967) 1617
8. P. B. Siegel, W. Weise, Phys. Rev. C **38** (1988) 2221
9. T. Waas, N. Kaiser, W. Weise, Phys. Lett. B **365** (1996) 12 *ibid* **379** (1996) 34.
10. E. Oset, A. Ramos, Nucl. Phys. A **635** (1998) 99
11. J.A. Oller, U.-G. Meißner, Phys. Lett B **500** (2001) 263
12. M. F. M. Lutz and E. E. Kolomeitsev, Nucl. Phys. A **700** (2002) 193
13. J.A. Oller, J. Prades and M. Verbeni, Phys. Rev. Lett. **95** (2005) 172502
14. D. Jido, J. A. Oller, E. Oset, A. Ramos, U.-G. Meißner, Nucl. Phys. A **725** (2003) 181
15. V. K. Magas, E. Oset, A. Ramos, Phys. Rev. Lett. **95** (2005) 052301
16. B. Borasoy, R. Nißler, W. Weise, Phys. Rev. Lett. **94** (2005) 213401
17. A. Sibirtsev, W. Cassing, Nucl. Phys. A **641** (1998) 476
18. M. Lutz, Phys. Lett. B **426** (1998) 12
19. A. Sibirtsev, W. Cassing, Phys. Rev. C **61** (2000) 057601.
20. A. Ramos *et al.*, Nucl. Phys. A **691** (2001) 258c
21. H. Heiselberg, M. Hjorts-Jensen, Phys. Rep. **328** (2000) 237
22. A. Cieply, E. Friedman, A. Gal, J. Mares, Nucl. Phys. A **696** (2001) 173
23. Y. Akaishi, T. Yamazaki, Phys. Rev. C **65** (2002) 044005
24. A. Dote, H. Horiuchi, Y. Akaishi, T. Yamazaki, Phys. Rev. C **70** (2004) 044313
25. A. Dote, Y. Akaishi, T. Yamazaki, Prog. Theor. Phys. Suppl. **156** (2004) 184
26. T. Suzuki *et al.*, Phys. Lett B **597** (2004) 263
27. Y. Akaishi, A. Dote, T. Yamazaki, Phys. Lett. B **613** (2005) 140
28. E. Oset and H. Toki, Phys. Rev. C **74** (2006) 015207
29. M. Agnello *et al.*, Phys. Rev. Lett. **94** (2005) 212303
30. V. K. Magas, E. Oset, A. Ramos, and H. Toki, Phys. Rev. C **74** (2006) 025206
31. A. Ramos , V. K. Magas, E. Oset, and H. Toki, Nucl. Phys. A **804** (2008) 219
32. R.C. Barrett, A. Deloff, Phys. Rev. C **60** (1999) 025201
33. A. Deloff, Phys. Rev. C **61** (2000) 024004
34. V.Yu. Grishina, L.A. Kondratyuk, M. Büscher, W. Cassing, Eur. Phys. J. A **21** (2004) 507
35. S.S. Kamalov, E. Oset, A. Ramos, Nucl. Phys. A **690** (2001) 494
36. U.-G. Meißner, U. Raha, and A. Rusetsky, Eur. Phys. J. C **47** (2006) 473
37. V.Yu. Grishina *et al.*, Eur. Phys. J. A **25** (2005) 159
38. V.Yu. Grishina, M. Büscher, and L.A. Kondratyuk, Phys. Rev. C **75** (2007) 015208
39. F. Bellemann *et al.*, Phys. Rev. C **75** (2007) 015204
40. E. Oset, J.A. Oller, U.-G. Meißner, Eur. Phys. J. A **18** (2003) 343
41. A. Dzyuba *et al.*, Eur. Phys. J. A 38 (2008) 1
42. M. L. Goldberger, K. M. Watson, *Collision Theory* (John Wiley and Sons, Inc., New York, London, Sidney 1964)
43. G. Fäldt, C. Wilkin, Nucl. Phys. A **587** (1995) 769
44. V.Yu. Grishina *et al.*, Phys. Lett. B **475** (2000) 9
45. V.N. Boitsov, L.A. Kondratyuk, V.B. Kopeliovich, Sov. J. Nucl. Phys., **16** (1973) 287
46. S. Wycech, A.M. Green, J.A. Niskanen, Phys. Rev. C **52** (1995) 544
47. V. Baru, E. Epelbaum, and A. Rusetsky, Eur. Phys. J. A, **42** (2009) 111
48. L. Kondratyuk, V. Grishina, and M. Büscher, *Proc. of the* 6th *Int. Conf. on Nuclear Physics at Storage Rings (STORI2005), Bonn, Germany, 23–26 May 2005* (eds. Forschungszentrums Jülich, Matter and Materials, vol. **30**, 2006, ISSN 1433-5506) 165
49. A. Ramos and E. Oset, Nucl. Phys. A **671** (2000) 481
50. S. Hirenzaki, Y. Okumura, H. Toki, E. Oset, and A. Ramos, Phys. Rev. C **61** (2000) 055205